Supporting Information

High Efficiency Nitrogen Doping and Single Atom Cobalt Anchoring via Supermolecules for Oxygen Reduction Electrocatalysis

Yuanyuan Chen,[1,#] Xiujuan Li,[1,#] Weijie Liao,[1] Lei Qiu,[2] Haitao Yang,[1] Lei Yao,[1,*] and Libo Deng[2,*]

[1]Shenzhen Key Laboratory of Special Functional Materials, Shenzhen Engineering Laboratory for Advanced Technology of Ceramics, Guangdong Research Center for Interfacial Engineering of Functional Materials, College of Materials Science and Engineering, Shenzhen University, Shenzhen 518060, P. R. China

[2] College of Chemistry and Environmental Engineering, Shenzhen University, Shenzhen 518060, China

*Corresponding authors: E-mail: lyao@szu.edu.cn, denglb@szu.edu.cn

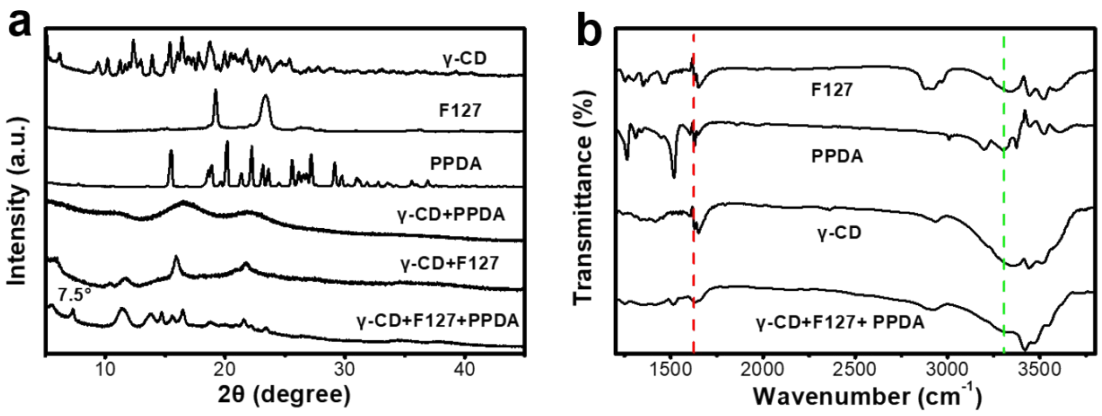

Fig. S1 Characterization of the freeze-dried samples obtained after the self-assembly of γ-CD, F127 and PPDA in different proportions. a) XRD patterns and b) FTIR spectra.

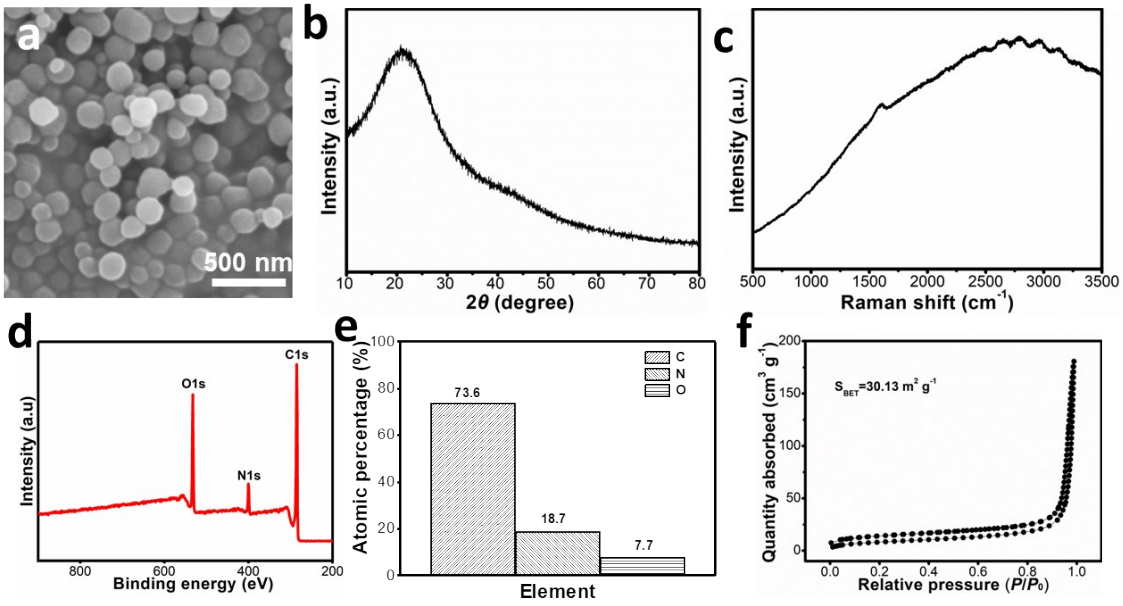

Fig. S2 Characterization of the sample obtained after the HTC of γ-CD/F127/ PPDA supramolecular complex. a) SEM image, b) XRD pattern, c) Raman spectrum, d) XPS spectrum, e) atomic percentages of different elements, and f) N_2 adsorption-desorption curves.

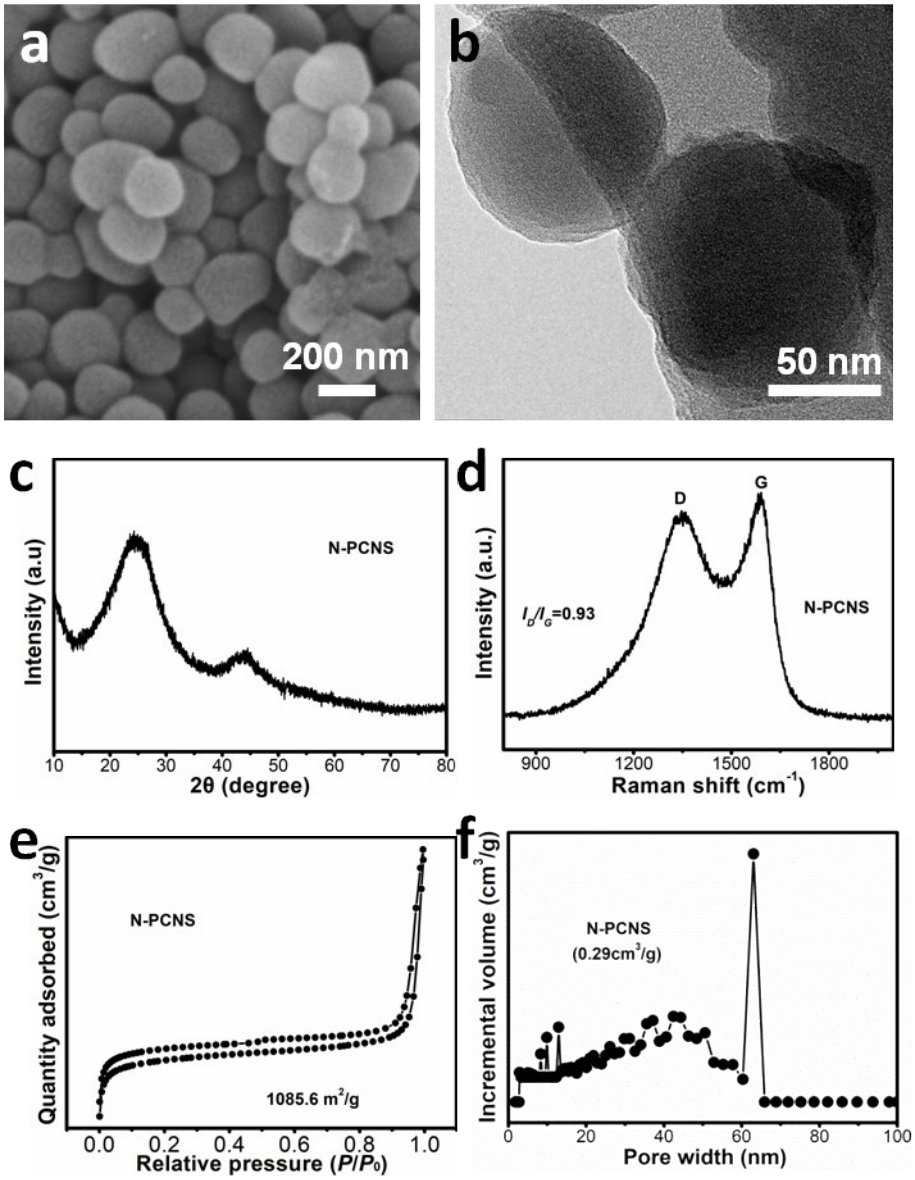

Fig. S3 Characterization of the N-PCNS. a) SEM image, b) TEM image, c) XRD pattern, d) Raman spectrum, e) N_2 adsorption-desorption curves, and f) pore size distribution.

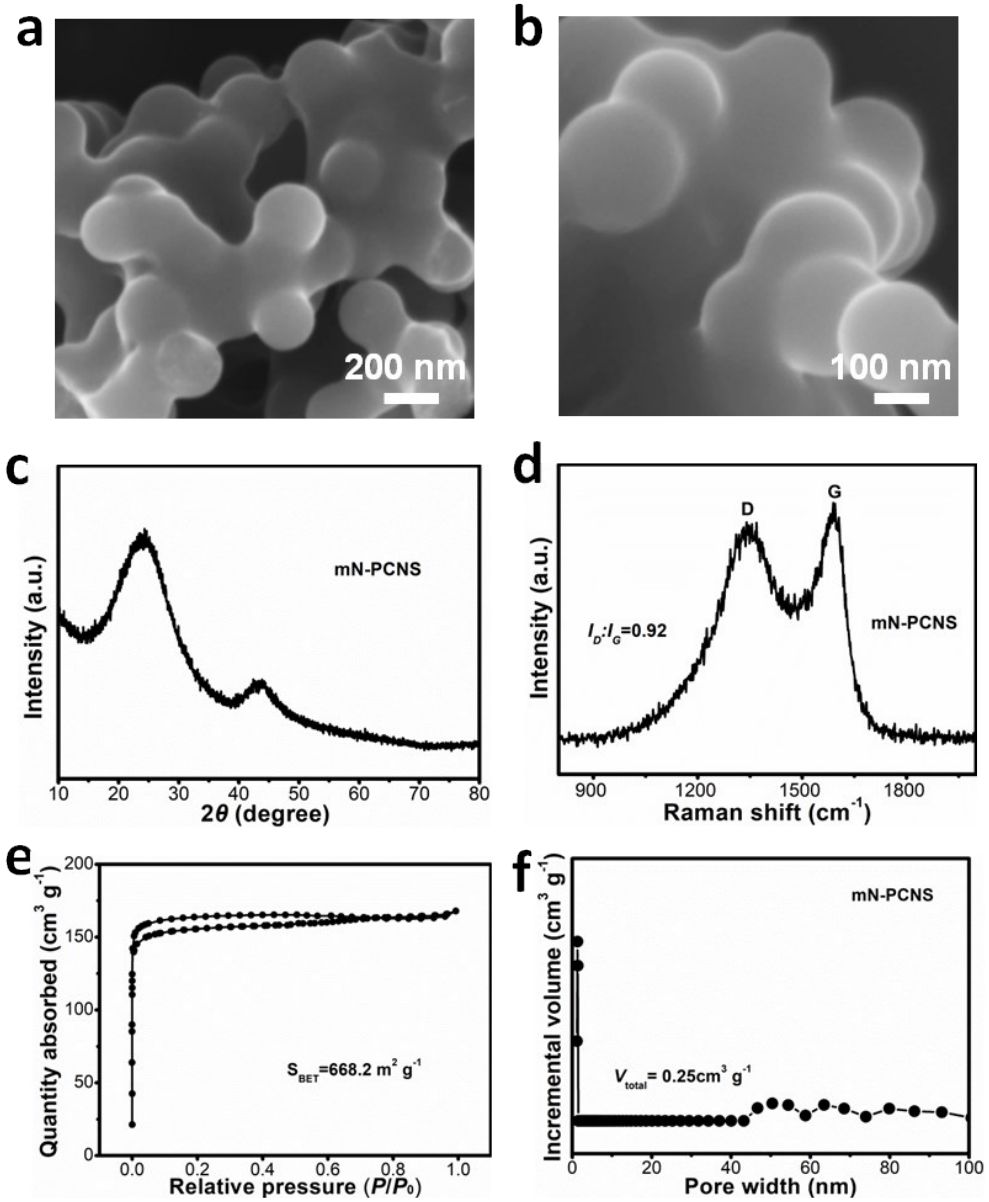

Fig. S4 Characterization of the mN-PCNS. a, b) SEM images, c) XRD pattern, d) Raman spectrum, e) N_2 adsorption-desorption curves, and f) pore size distribution.

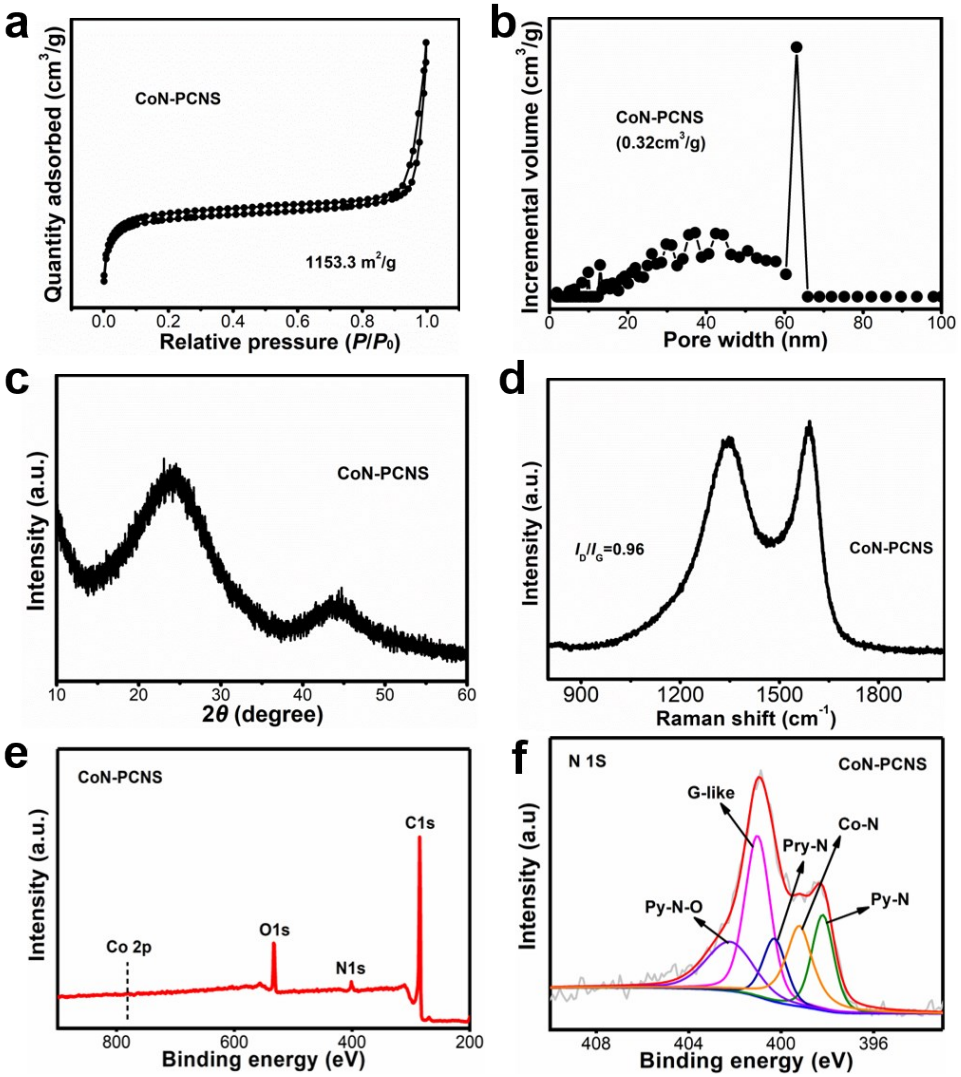

Fig. S5 Characterization of the CoN-PCNS: a) N_2 adsorption-desorption curves, b) pore size distribution curve, c) XRD pattern, d) Raman spectrum, e) XPS survey spectrum, and f) high-resolution N 1s spectrum.

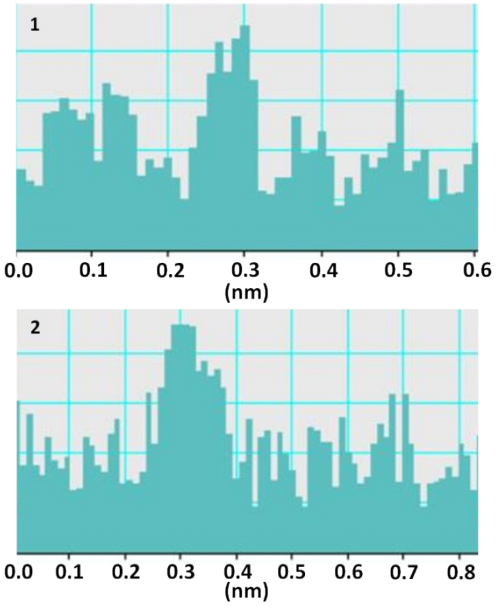

Fig. S6 The height profiles of single Co atoms from two regions in CoN-PCNS.

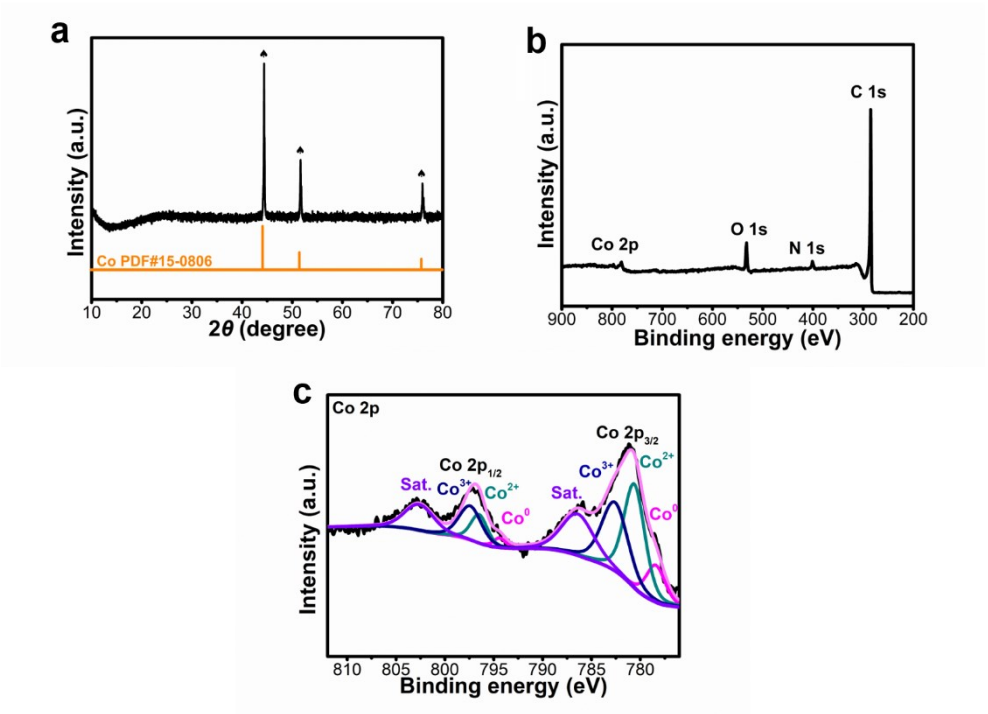

Fig. S7 a) XRD pattern, b) XPS survey spectrum and c) high-resolution Co 2p spectrum for the pyrolyzed CoN-PCNS before acid leaching.

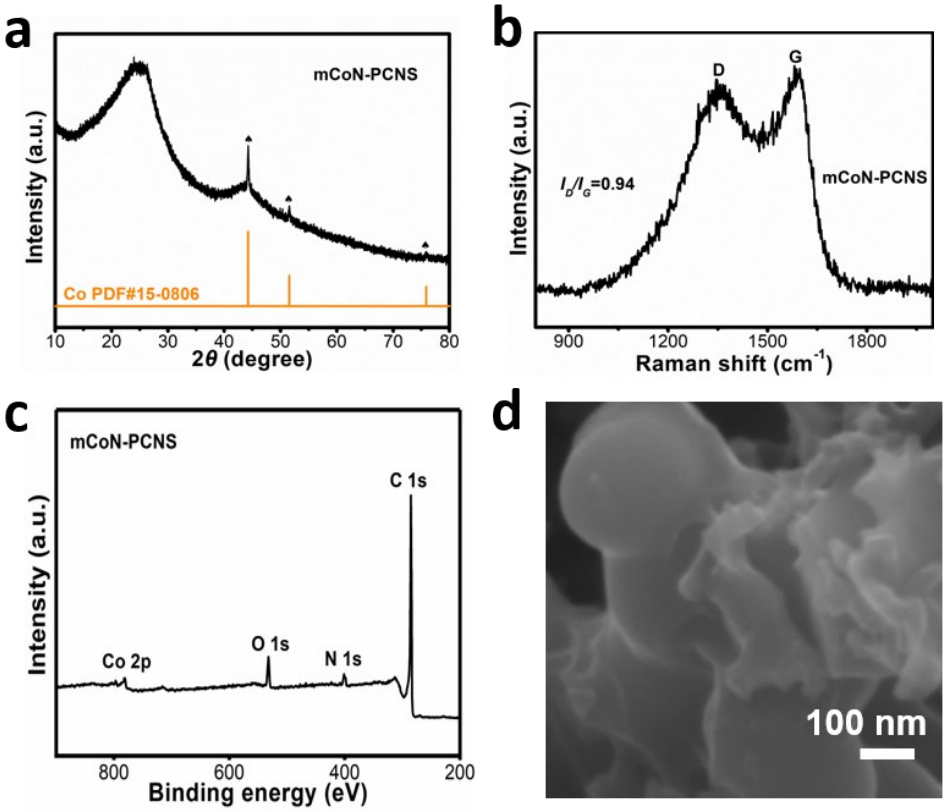

Fig. S8 Characterization of the mCoN-PCNS: a) XRD pattern, b) Raman spectrum, c) XPS spectrum, and d) SEM image.

A number of transion metals, including Fe, Ni and Cu were incorporated into the carbon matrix to prepare single atomic catalysts. XRD characterization suggests that there are no metal phases in the catalysts (Fig. S9). Furthermore, HAADF-STEM images showed numerous bright dots in all catalysts (Fig. S10), indicating the atomic states of metals.

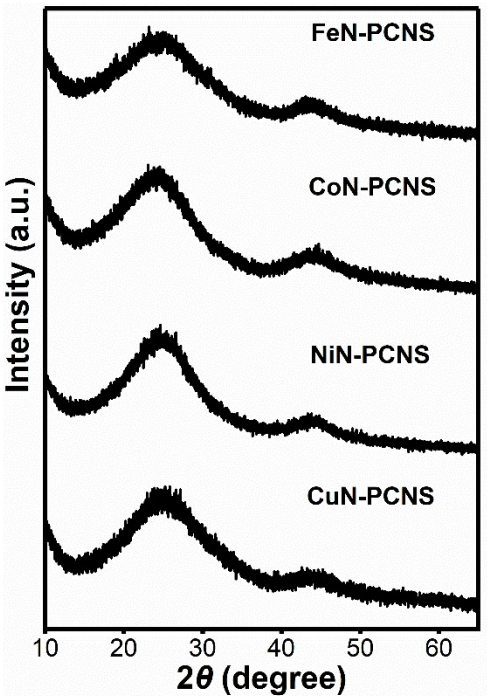

Fig. S9 XRD patterns of MN-PCNS (M = Fe, Co, Ni and Cu)

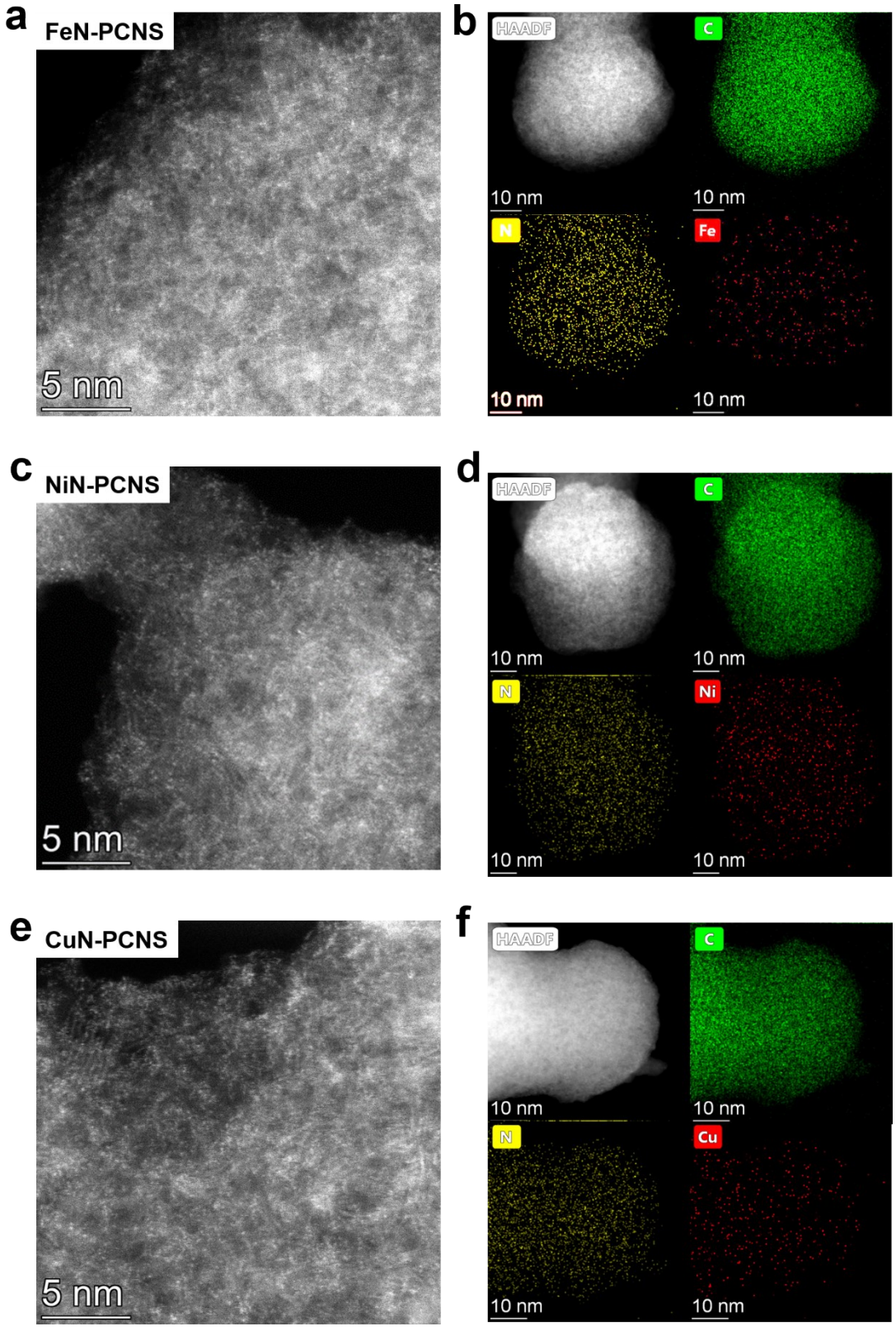

Fig. S10 Aberration-corrected HAADF-STEM images of the MN-PCNS (M = Fe, Ni and Cu) and the corresponding EDX maps showing distribution of the metal atoms.

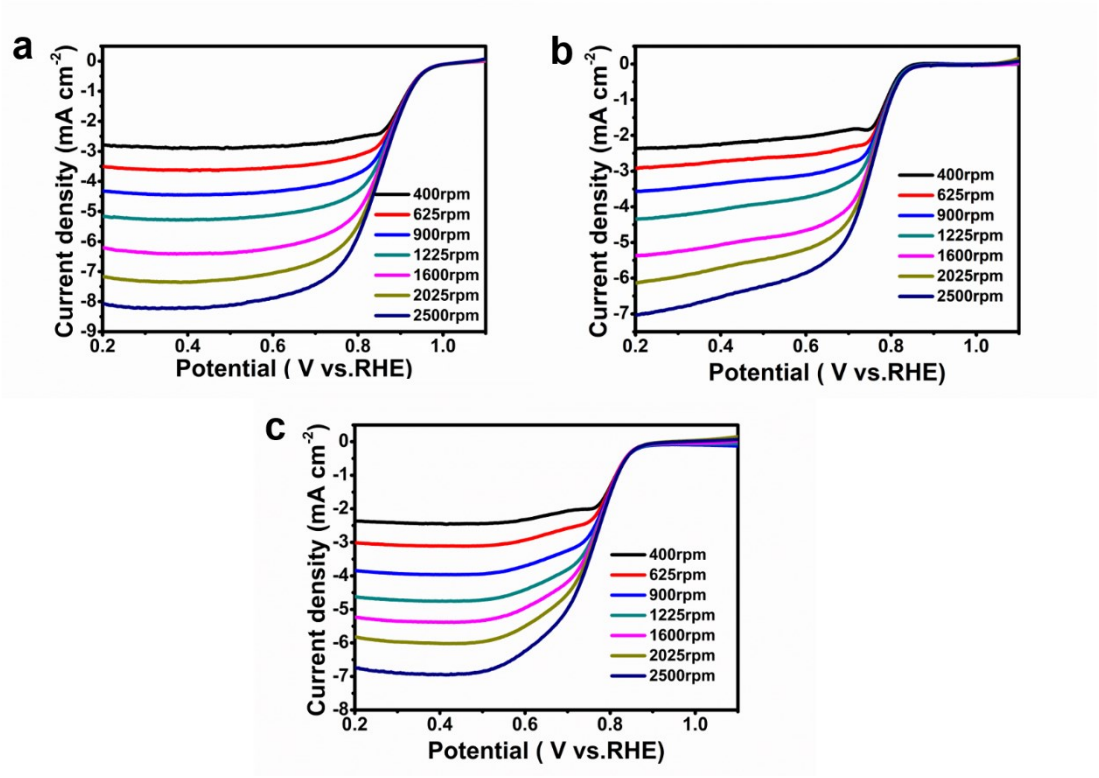

Fig. S11 LSV curves for the MN-PCNS tested in 0.1 M KOH: a) FeN-PCNS, b) NiN-PCNS, and c) CuN-PCNS

The effect of pyrolysis temperature on the structure and performance of CoN-PCNS catalysts was investigated. Raman spectroscopic characterization suggested the I_D/I_G ratio of the carbon matrix increases with the pyrolysis temperature, indicating the increasingly graphitization degree, but the lateral crystal size (L_a) for all these carbons were below 2 nm. The small microcrystalline feature was further corrobrated with XRD characterization (Fig. S12b). LSV curves acquired at different rotating speeds are shown in Fig. S13. Furthermore, LSV curves at 1600 rpm for all samples, which allows a quick comparison of the performance, are shown in Fig. S14. The performance (with the onset potential and limiting current as the descriptors) improves with the pyrolysis temperature in the range of 700 ~900 °C, due to the increasingly graphitization degree which enhances the conductivity. Further increasing the temperature resulted in an inferior performance, which might be attributed to the collapse of micropores at a high temperature.

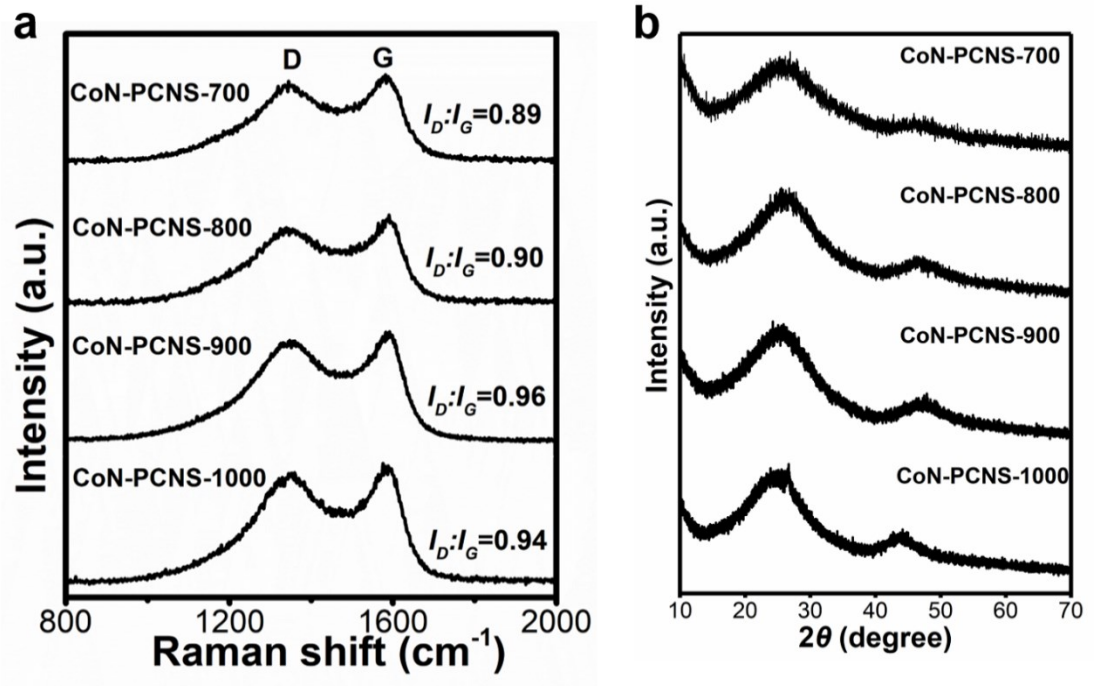

Fig. S12 a) Raman spectra and b) XRD patterns for CoN-PCNS pyrolyzed at different temperatures.

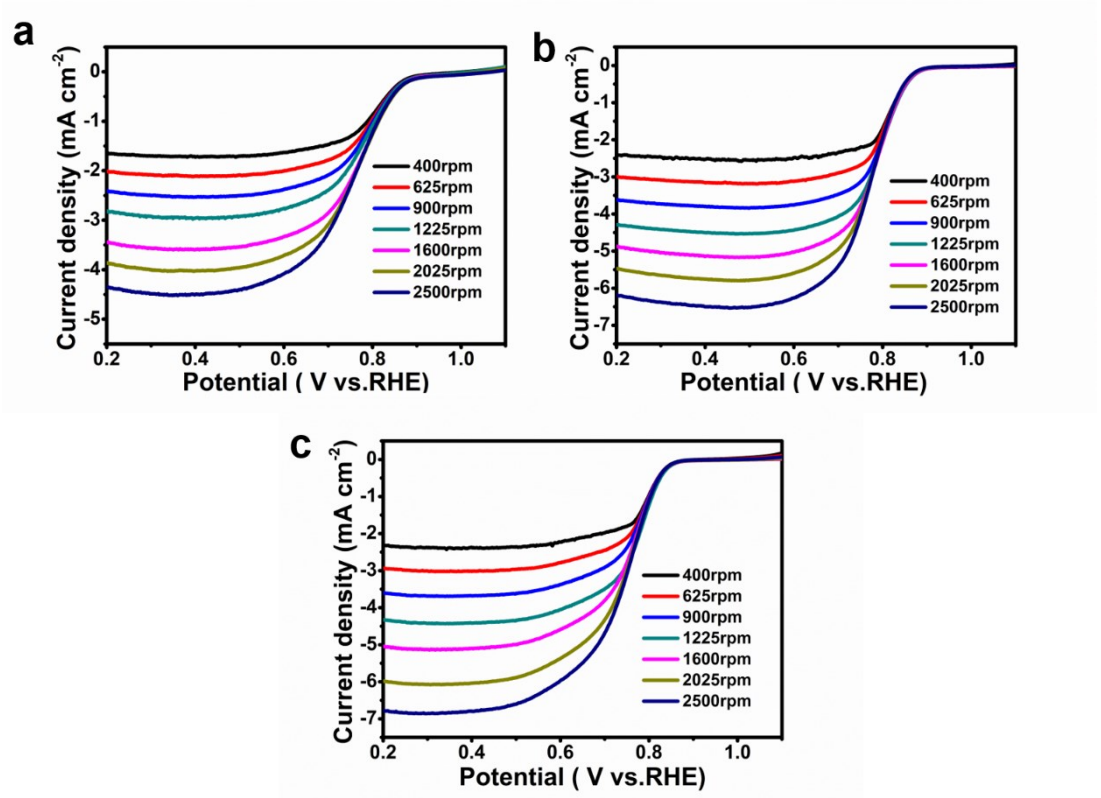

Fig. S13 LSV curves for the CoN-PCNS pyrolyzed at different temperatures and tested in 0.1 M KOH: a) 700 °C, b) 800 °C, and c) 1000 °C.

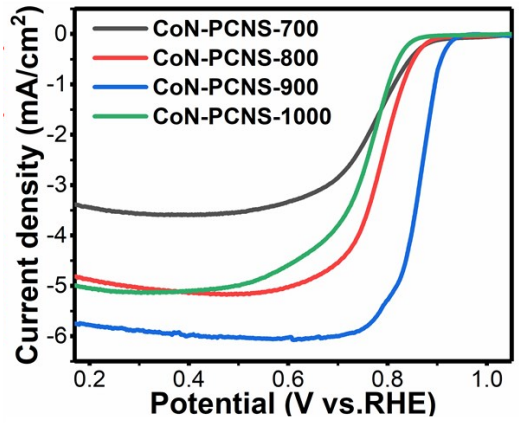

Fig. 14 LSV curves acquired at 1600 rpm in 0.1 M KOH for CoN-PCNS pyrolyzed at different temperatures.

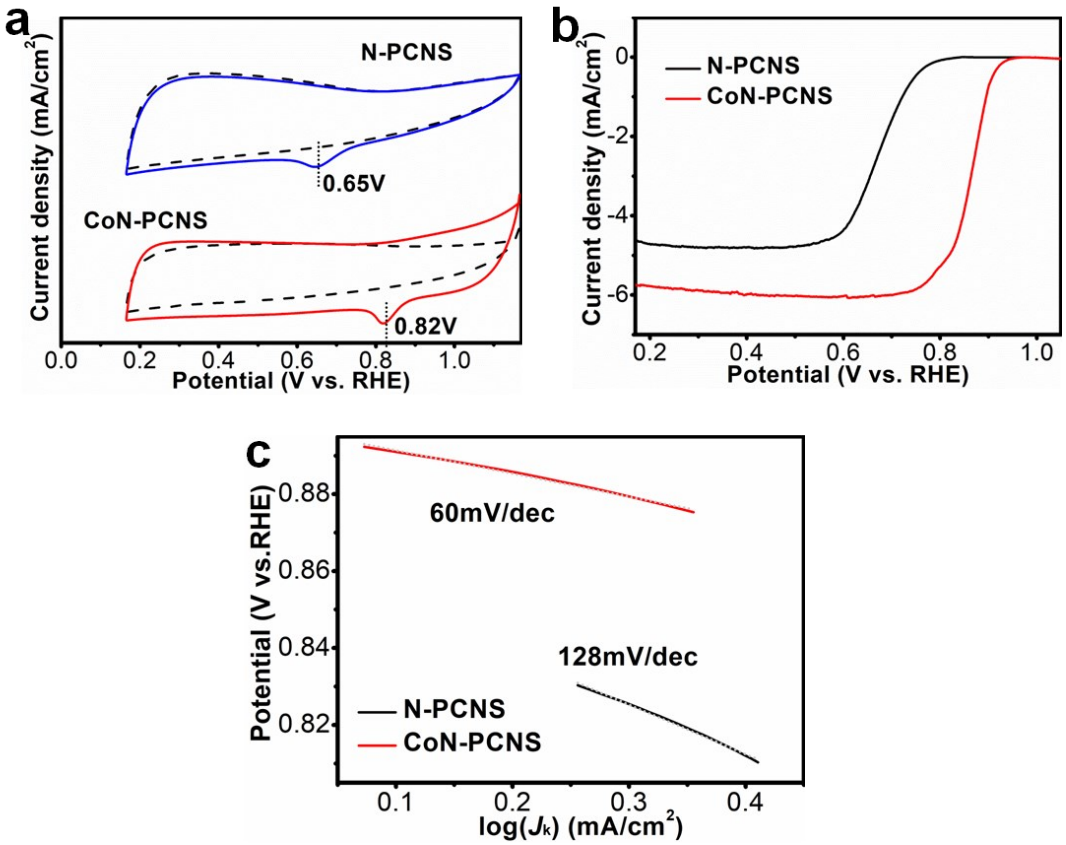

Fig. S15 a) CV curves, b) LSV curves acquired at 1600 rpm, and c) Tafel plots for the N-PCNS and CoN-PCNS.

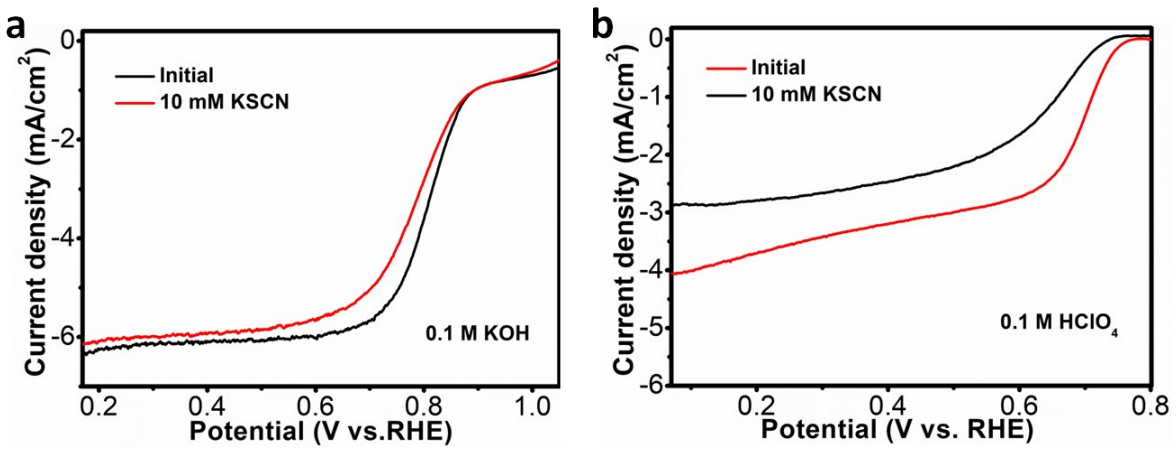

Fig. S16 ORR polarization curves for CoN-PCNS poisoned by SCN^- in a) 0.1 M KOH and b) 0.1 M $HClO_4$.

Table S1 The compositions of the pyrolyzed nanospheres as determined by XPS

Catalysts	N (at.%)	C (at.%)	O (at.%)	Co (at.%)
N-PCNS	3.30	87.40	9.30	0
mN-PCNS	2.24	90.90	6.86	0
CoN-PCNS	3.57	85.21	11.30	0.20
mCoN-PCNS	4.79	86.92	7.13	1.16

Table S2 EXAFS fitting parameters at the Co K-edge) for various samples ($S_0^2 = 0.776$)

Sample	Shell	N[a]	R(Å)[b]	σ^2(Å^2)[c]	ΔE_0 (eV)d	R factor
Co foil	Co-Co	12	2.49	0.0063	7.2	0.0004
	Co-O	5.1	2.06	0.0101		
CoO	Co-Co	13.5	2.99	0.0095	-3.6	0.0004
	Co-O	6.2	3.66	0.0101		
CoPc	Co-N	4.0	1.91	0.0013	6.2	0.0078
CoN-PCNS	Co-N	1.2	1.83	0.0028	-1.8	0.0001
	Co-N	2.5	2.01	0.0028		

[a]N: coordination number; [b]R: bond distance; [c]σ^2: Debye-Waller factor; [d]ΔE_0: the inner potential correction. R factor: goodness of fit. S_0^2 was set to 0.776, based on fitting experimental EXAFS data obtained from a Co foil reference and fixing CN to a known crystallographic value.

Table S3 Comparison of the electrochemical performance of the CoN-PCNS catalyst with those previously reported for other materials

Electrocatalysts	N (%)	Co (%)	E_{onset} (V vs. RHE)	$E_{1/2}$ (V vs. RHE)	Ref.
CN_x-Co-1000	1.4 at.%	1.2 at.%	0.92	0.823	[1]
Co@SACo-N-C	4.9 wt.%	1.95 wt.%	0.92	0.778	[2]
Co-NHC-900	-	1.25 wt.%	-	0.85	[3]
CoNC	4.8 at.%	1.52 at.%	0.9	0.81	[4]
CoO_x@NGCR	4.3 at.%	-	0.91	0.8	[5]
NBSCP	7.5 at.%	0.46 at.%	-	0.836	[6]
Co-N/CNFs	2.3 at.%	0.66 at.%	0.92	0.82	[7]
N/Co/CMK-3 plate	1.8 at.%	0.28 at.%	0.88	0.77	[8]
CoN-PCNS	3.6 at.%	0.2 at.%	0.93	0.85	This work
20Co-NC-1100	3.6 at.%	0.3 at.%	0.93	0.8	[9]

Table S4 Comparison of the electrochemical performances of the N-PCNS, CoN-PCNS and mCoN-PCNS

Samples	E_{onset} **(V vs. RHE)**	$E_{½}$ **(V vs. RHE)**	J_{limit} **(mA/cm^2)**
N-PCNS	0.80	0.70	-4.67
CoN-PCNS	0.93	0.86	-5.74
mCoN-PCNS	0.84	0.73	-3.10

Table S5 Surface energy values for various intermediate products adsorbed on the surfaces of various catalysts

	$E_{\text{N-PCNS}}$ (eV)	$E_{\text{CoN-PCNS}}$ (eV)
Surface	-434.657801	-444.7412951
Surface+OOH	-448.529494	-459.1032198
Surface+O	-439.151208	-449.553168
Surface+OH	-444.291205	-454.9161713

References

1. Y. Lu, X. Wen, X. Chen, P.K. Chu, T. Tang, E. Mijowska, Nitrogen-doped Porous Carbon Embedded with Cobalt Nanoparticles for Excellent Oxygen Reduction Reaction. Journal of Colloid and Interface Science. J. Colloid Interface Sci. **546**, 344-350 (2019).
2. Q. Chen, S. Han, K. Mao, C. Chen, L. Yang, Z. Zou, M. Gu, Z. Hu, H. Yang, Co Nanoparticle Embedded in Atomically-dispersed Co-N-C Nanofibers for Oxygen Reduction with High Activity and Remarkable Durability. Nano Energy **52**, 485-493 (2018).
3. K. Hu, L. Tao, D. Liu, J. Huo, S. Wang, Sulfur-Doped Fe/N/C Nanosheets as Highly Efficient Electrocatalysts for Oxygen Reduction Reaction. ACS Appl. Mater. Interfaces **8**, 19379-19385 (2016).
4. X. Tang, H.Y. Ng, Cobalt and nitrogen-doped carbon catalysts for enhanced oxygen reduction and power production in microbial fuel cells. Electrochim. Acta **247**, 193-199 (2017).
5. C.-C. Weng, J.-T. Ren, Z.-P. Hu, Z.-Y. Yuan, Nitrogen-Doped Defect-Rich Graphitic Carbon Nanorings with CoO_x Nanoparticles as Highly Efficient Electrocatalyst for Oxygen Electrochemistry. ACS Sustain. Chem. Eng. **6**, 15811-15821 (2018).
6. D.W. Lee, J.H. Jang, I. Jang, Y.S. Kang, S. Jang, K.Y. Lee, J.H. Jang, H.J. Kim, S.J. Yoo, Bio-Derived Co_2P Nanoparticles Supported on Nitrogen-Doped Carbon as Promising Oxygen Reduction Reaction Electrocatalyst for Anion Exchange Membrane Fuel Cells. Small **15**, 1902090 (2019).
7. Q. Cheng, L. Yang, L. Zou, Z. Zou, C. Chen, Z. Hu, H. Yang, Single Cobalt Atom and N Codoped Carbon Nanofibers as Highly Durable Electrocatalyst for Oxygen Reduction Reaction. ACS Catal. **7**, 6864-6871 (2017).
8. V.M. Bau, X. Bo,L. Guo, Nitrogen-doped Cobalt Nanoparticles/nitrogen-doped Plate-like Ordered Mesoporous Carbons Composites as Noble-metal Free Electrocatalysts for Oxygen Reduction Reaction. J. Energy Chem. **26**, 63-71 (2017).
9. Y.-E. Miao, J. Yan, Y. Ouyang, H. Lu, F. Lai, Y. Wu,T. Liu, A Bio-inspired N-doped Porous Carbon Electrocatalyst with Hierarchical Superstructure for Efficient Oxygen Reduction Reaction. Appl. Surf. Sci. **443**, 266-273 (2018).